

3D ad-hoc sensor networks based localization and risk assessment of buried landfill gas source

Saurav Mitra, Siddhartha P. Duttagupta, Kushal Tuckley, Samsul Ekram

Abstract—Anaerobic decomposition of landfill garbage produces gases like CH_4 and H_2S at subsurface. These gases diffuse through the foundation and come out to pollute the indoor building environment above. CH_4 is highly flammable and causes explosion whereas H_2S causes equipment failure and significant pulmonary ailments in human beings over long term exposure. This work focuses on 3D ad-hoc wireless sensor network (WSN) based localization and risk assessment of such a gas source buried at subsurface. Experiments are performed to emulate the gas diffusion process at underground. Experiments also help to determine gas propagation constants over the surface. Higher precision of the three-step maximum likelihood (ML) based source localization method enhances the accuracy of source risk assessment process. Simulation results indicate that the proposed localization algorithms with limited sensor node mobility offer higher accuracy of estimation using lesser network resources. Finally, we propose an analysis for remote source concentration measurement. This help estimate severity of threat possessed by the buried landfill gas source. Also a method is proposed for 3D ad-hoc WSN based source location estimation with obstructed paths for surface gas propagation.

Keywords—Buried landfill source, gas source localization, risk assessment, 3D ad-hoc wireless sensor networks.

I. INTRODUCTION

DUE to space crunch in megacities, new buildings are constructed over not so old former garbage landfill sites. Anaerobic decomposition of the wastes at moist and humid subsurface produce hazardous gases like CH_4 , CO_2 , H_2S , benzene, trichloroethene, toluene, xylene etc. Under the effect of negative pressure, these gases diffuse through the soil and concrete foundation and come out to pollute the building

Manuscript received October 28, 2011. This work is supported by the Crompton Greaves Limited, Kanjurmarg, Mumbai, India.

Saurav Mitra is a Ph. D. research scholar with the Indian Institute of Technology Bombay, Powai, Mumbai, Maharashtra, India (phone: +91-22-2576-7866; fax: +91-22-2572-3707; e-mail: sauravm@ee.iitb.ac.in).

Siddhartha P. Duttagupta is assistant professor with the Indian Institute of Technology Bombay, Powai, Mumbai, Maharashtra, India (phone: +91-22-2576-7866; fax: +91-22-2572-3707; e-mail: sdgupta@ee.iitb.ac.in).

Kushal Tuckley is director and chief of research and development of AGV Systems Pvt. Ltd., Goregaon (E), Mumbai, MH, India (Phone: +91-22-2685-3634; fax: +91-22-2572-3707; e-mail: kushal.tuckley@agv-systems.in).

Samsul Ekram is assistant general manager of Crompton Greaves Limited, Kanjurmarg, Mumbai, Maharashtra, India (Phone: +91-22-6755-9083; fax: +91-22-6755-9008; e-mail: samsul.ekram@cgglobal.com).

environment above [1]-[3]. In Grand Riviera Princess Hotel at Playa Del Carmen, Mexico, accumulation of methane from nearby swamp caused huge explosion at basement. It rendered many deaths and severe financial damage [4]. In another incident at Malad office of Mindspace BPO, Mumbai subsurface H_2S infiltrated through the floor and led to incessant crashing of computers, and electrical equipments [1]. In less aerated offices, industries, and residential buildings, the ailing effects of such gases on human beings can create nausea, headache, and serious lung diseases like asthma, bronchitis, and even cancer [2]. In such scenarios, it is of immediate necessity to track the source of contamination and identify the degrees of threat that the gas sources possess towards employees and equipments within [5]. This helps the proper authorities to deal with the crisis and restraining the hazardous effects through preventive measures.

Landfill gases (LFG) generally contains CO_2 and CH_4 as dominant emission elements (45-50% each), and H_2S (3-5%) and other volatile organic compounds (VOC-1%) as trace elements. For its distinct rotten smell, presence of H_2S in the indoor environment is easily felt even for ppm level concentration. But CH_4 concentration determination at source is highly challenging as CH_4 is odorless and colorless. 5 to 15% of CH_4 in indoor environment produces a highly flammable mixture in presence of O_2 /air [2]. Over a large surface area, manual localization of such gas sources and remote monitoring of gas effusion rate would be highly cumbersome and ineffectual. But with the help of dedicated self-powered wireless sensor nodes, this type of critical event monitoring becomes lot easy. These multi sensor nodes when networked together can provide quick real-time detection, identification and threat assessment with higher accuracy. Examples include monitoring of the accidental spillage of toxic waste by ships, factories etc that contaminate the sea and the air, early detection of fires, nuclear radiation monitoring, and other environmental monitoring and so on [6].

Environmental monitoring and toxic gas source localization is one of the most promising fields of research since it enhances human safety in adverse residential and industrial environments [7]. One of the common issues has been that most detection of chemicals with mobile robots has been based on experimental setups where the distance between the source and the sensor following an odor trail has been minimized to limit the influence of turbulent transport [8]-[10]. In many cases mobile robots are also used for localization of toxic chemical plume source for explosive

detection [8], [11]-[13]. Robot based biologically-inspired search strategy for locating odor source is also reported which solves the problems of repetitive search [14]. But, robot based systems have some inherent shortcomings as such systems cannot function satisfactorily in all types of non-cooperative environments of factory or mines. Moreover if the monitoring area is too big and there are many obstacles in the site, the robots face big problems. In addition, high cost and energy consumption of the robot based systems also cannot be ignored [15]. Sensor network based schemes on the other hand can be planned to use in most of the scenarios where mobile robots cannot be deployed. Sensor networks can instantly detect the plume source whereas the mobile robot based scanning is more time consuming [6], [16]. Sensor network is more flexible in terms of reconfiguration of data routing path in case of few node failures [6]. Moreover, a dedicated sensor network does not require thorough human attention during target detection. Modeling for plume source based location estimation is explained in detail in [11]-[13]. The energy model, routing protocols, topology, and network connectivity related issues of H₂S monitoring using sensor networks has been explored in [17]. Remote threat estimation of the toxic H₂S source explained here can be very useful in oil and gas resource industries [16].

Main contribution in this paper is determination of gravity of threat of a buried subsurface hazardous gas source in real time. The novel 3D sensor node configuration proposed here can satisfactorily perform source risk assessment even when the gas propagation paths in certain directions from source are blocked by obstacles. The three step source localization strategy uses maximum likelihood (ML) estimation technique. In our simulations, the initial localization is carried out considering gas concentration readings from all sensor nodes. Next, refined source location information is obtained with strategically chosen lesser number of sensor nodes. Finally, with limited directive mobility applied to the subset sensor nodes, highly precise source localization is achieved. The proposed source localization criteria give highly accurate result with limited network resources. Finally, the proportionate emission rate of noxious H₂S at source with respect to CH₄ emission is remotely estimated using a single closest sensor node. This is also a novel contribution. The criteria help estimate lethality of the source and criteria for intervention.

The paper is organized as follows. In Section II, we present an equivalent experimental set up that emulates subsurface multiple path gas diffusion process. Surface gas propagation constants for CH₄ and H₂S are also determined from this experiment. In Section III, we present the model and assumptions for CH₄ propagation within the target area. The common criterion for determination of theoretical lower bound of source estimation error is also explained in this section. The criteria for sensor node placement, subset node selection, limited node mobility, and remote gas effusion rate determination at source are explained in detail in section IV. In Section V, we present a representative case for three

dimensional sensor node based gas source localization process and related assumptions. Section VI contains the simulation results for above explained cases. We conclude with Section VII where plans for future works are presented.

II. EXPERIMENTAL SETUP

The water-cement ratio in soil and basement concrete is increased due to higher moisture concentration at subsurface. This accelerates pore formation in concrete which in turn facilitates gas diffusion through it. The nature of migration of gases through such porous media is the subject of extensive literature and has been studied in several occasions. The fundamental mechanism of gas migration is due to an imposed pressure gradient (bulk or preamble) and composition gradient (diffusion migration) [18], [19]. The mixture of subsurface gases when effuse through the surface crack follows Graham's law of effusion. According to this law, the rate of gas effusion from the point of leak is inversely proportional to the square root of its molar mass. Hence CH₄ release rate is 1.46 times than that of H₂S. Being lighter, CH₄ propagates isotropically whereas heavier H₂S spreads slowly along with the floor. It makes CH₄ a more suitable element for 2D and 3D gas source localization than H₂S. The one dimensional molecular gas diffusion process is described by Fick's first law –

$$J(x) = -D \cdot (dc/dx) \quad (1)$$

where $J(x)$ is the gas flux, dc/dx is the gradient of concentration and D is the gas diffusion coefficient.

An experimental test bed of dimension 3×1×1.2 cubic meters emulates the subsurface gas diffusion process, Fig. 1. The cubical box is divided into upper (surface) and lower (subsurface) chambers which are separated by solidified porous hydrated cement paste layer or hcp barrier (soil-concrete foundation). Three intentionally induced cracks in the hcp layer were three dominant effusion points which created bias in gas diffusion. Three multisensor nodes were designed with both CH₄ (MQ4 with sensitivity 200-10000 ppm) and H₂S sensors (ME4 with sensitivity 0-200 ppm) to obtain gas concentration readings at various points in the upper chamber. For CH₄ concentration in the upper chamber, we observed a combined almost Gaussian pattern in the left side around effusion points 1 and 2. A Gaussian pattern around effusion point 3 was observed in the right side of the chamber, Fig. 2. The proximity of effusion points 1, and 2 caused the single combined diffusion pattern in the left side. During experiment for a lone CH₄ source we observed that gas concentration varies inversely with power of 2.3 of the Euclidean distance between source and the measuring point at room temperature of 30°C. For H₂S, this constant was observed to be 2.6. The value of gas propagation constant is a function of relative humidity, ambient temperature, and gas partial pressure at source etc [20]. These findings decide the criteria for 2D and 3D sensor placement towards obtaining highest sensitivity and highest source localization accuracy in real scenario.

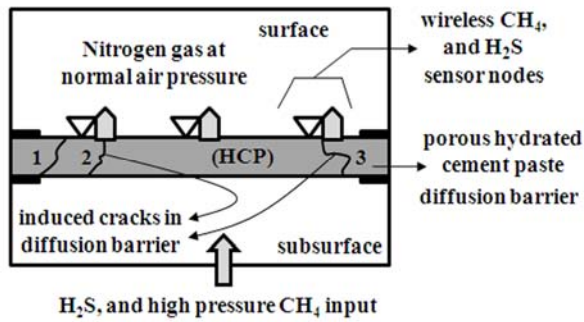


Fig. 1 test bed emulates the process of CH₄, and H₂S gas diffusion

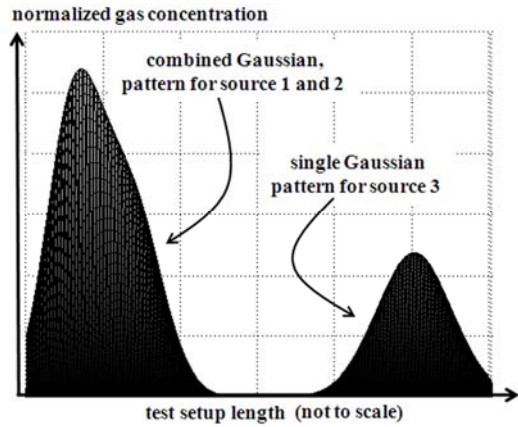


Fig. 2 CH₄ concentration pattern at upper chamber

Fig. 3 shows a case with three CH₄ sources. Q₁ is the mean for a combined CH₄ sources and Q₂ is an independent source. Sensor kept at A would sense combined CH₄ concentration- for Q₁, concentration at A = 1200 ppm / 2^{2.3} = 256 ppm for Q₂, concentration at A = 300 ppm / 2^{2.3} = 61 ppm. As the minimum sensing threshold for MQ4 is 200 ppm, the sensor at A would detect Q₁ source with higher accuracy.

III. CH₄ PROPAGATION MODEL AND ESTIMATION ERROR

Over a large target area, it is really a challenging job to estimate the domain of CH₄ effusion point in 2D and 3D environment. It is assumed that both CH₄ and H₂S effuse from the same source at a constant rate. Initially, through proximity measurements, precise CH₄ effusion region estimation is obtained. Using this information and the gas propagation constants as apriori, CH₄ to H₂S concentration ratio at source is estimated consequently. Here, CH₄ acts as proxy for H₂S source location estimation.

A. CH₄ Propagation Model in Indoor Environment

The gas propagation and sensing model explained in this section does not account for potential impacts of wind flow and obstacles in the field. N numbers of CH₄ sensor nodes are assumed to be present in the target area. Also assumed that the concentrations of the K number of CH₄ sources (when K>1) will be linearly superimposed without any interaction on all the CH₄ sensors [21]. The concentration signal received at the

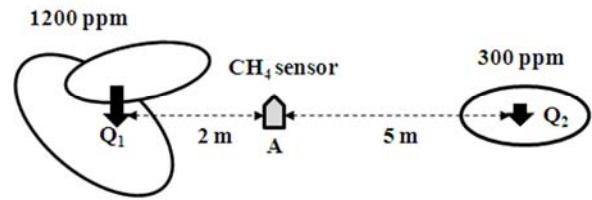


Fig. 3 representative case for sensing multiple gas sources at distance

i^{th} sensor node ($i=1, 2, \dots, N$) during discrete time interval n is

$$x_i(n) = s_i(n) + v_i(n) \quad (2)$$

where $s_i(n)$ is the actual CH₄ concentration without noise and measured at i^{th} sensor node due to all CH₄ sources. $v_i(n)$ is the background additive white Gaussian noise (AWGN). If T is the time window over which N sensor nodes pick up CH₄ concentration reading and if M is the number of sample points per time window, then $T = M / f_s$, where f_s is the sampling frequency [21]. $R_i(t)$ or the average CH₄ concentration measurements over the time window $[t-T/2, t+T/2]$ is the addition of signal energy $[R_{si}(t)]$ and noise energy $[\varepsilon_i(t)]$ as given below –

$$R_i(t) = \frac{1}{M} \sum_{n=(t-T/2)f_s}^{n=(t+T/2)f_s} s_i^2(n) + \frac{1}{M} \sum_{n=(t-T/2)f_s}^{n=(t+T/2)f_s} v_i^2(n) \quad (3)$$

CH₄ concentration information received by i^{th} sensor node at time index t can be expressed as [21] –

$$R_i(t) = R_{si}(t) + \varepsilon_i(t) = g_i \sum_{k=1}^K \frac{S_k(t)}{d_{ik}^\alpha} + \varepsilon_i(t) \quad (4)$$

where, $S_k(t)$ is the signal concentration energy at unit distance away from the k^{th} source, d_{ik} is the Euclidean distance between the i^{th} sensor and the k^{th} source, α is propagation constant of CH₄ in the media, $r_i = [x_i, y_i]^T$ is the known location of the i^{th} sensor node, and $\rho_k = [u_k, v_k]^T$ is the unknown location of the k^{th} source (ρ_k is to be estimated). The term g_i is the gain factor of the i^{th} sensor node. The square of the background noise $v_i^2(n)$ will have a Chi-Square distribution with mean equal to $E[v_i^2(n)] = \zeta_i^2$ and variance equal to $2\zeta_i^4/M$. If M is sufficiently large (> 30) then according to the Central Limiting theorem, ε_i can be approximated with a normal distribution $\varepsilon_i \sim N(\zeta_i^2, 2\zeta_i^4/M)$. For convenience, later in derivation, μ_i and σ_i^2 are denoted as ζ_i^2 and $2\zeta_i^4/M$ respectively [21]. The validity of this 2D CH₄ propagation model in an indoor environment has been verified with simulation results in section VI.

B. ML Estimation Based Source Localization Model

Source location determination for various environmental parameter monitoring has produced vast literatures over the years. For accurate detection of mineral distributions in the study area by means of the spectral analysis of Hyperion data has been reported [22]. But the system cost of image based and mobile robot systems are too high for small scale

applications. RF based source localization is comparatively cheaper solution for such problems in an indoor environment [23]. The gas source location estimation problem as explained in this paper is based on a single set of superimposed reading of gas concentrations at different sensor nodes with known coordinates. Time index T is omitted for brevity. The matrices for initial and coarse source localization are

$$\begin{aligned}
 H &= GD \\
 S &= [S_1 \ S_2 \ \dots \ S_K]^T \\
 \xi &= [\xi_1 \ \xi_2 \ \dots \ \xi_N]^T \\
 Z &= \left[\begin{array}{cccc} R_1 - \mu_1 & R_2 - \mu_2 & \dots & R_N - \mu_N \\ \sigma_1 & \sigma_2 & \dots & \sigma_N \end{array} \right]^T \\
 D &= \begin{bmatrix} \frac{1}{d_{11}^\alpha} & \frac{1}{d_{12}^\alpha} & \dots & \frac{1}{d_{1K}^\alpha} \\ \frac{1}{d_{21}^\alpha} & \frac{1}{d_{22}^\alpha} & \dots & \frac{1}{d_{2K}^\alpha} \\ \vdots & \vdots & \ddots & \vdots \\ \frac{1}{d_{N1}^\alpha} & \frac{1}{d_{N2}^\alpha} & \dots & \frac{1}{d_{NK}^\alpha} \end{bmatrix} \\
 G &= \text{diag} \left[\frac{g_1}{\sigma_1} \ \frac{g_2}{\sigma_2} \ \dots \ \frac{g_N}{\sigma_N} \right]
 \end{aligned} \quad (5)$$

where $\xi_i = (\varepsilon_i - \mu_i) / \sigma_i \sim N(0,1)$ are independent Gaussian random variables. Equation, (4) can be represented as

$$Z = GDS + \xi = HS + \xi. \quad (6)$$

The joint probability density function of Z is expressed as

$$f(Z|\theta) = (2\pi)^{\frac{N}{2}} \exp\left\{-\frac{1}{2}(Z - HS)^T(Z - HS)\right\}, \quad (7)$$

$$\text{where, } \theta = [\rho_1^T \ \rho_2^T \ \dots \ \rho_K^T \ S_1 \ S_2 \ \dots \ S_K]^T, \quad (8)$$

is the vector for unknown parameters. The negative likelihood objective function can be expressed as

$$l(\theta) = \|Z - GDS\|^2. \quad (9)$$

Thus the maximum likelihood parameter estimation of θ is obtained by minimizing $l(\theta)$ in (9). To minimize $l(\theta)$ for CH₄ source (K=1) [24], solution must lie on stationary point where

$$\frac{\partial l(\theta)}{\partial S} = 0 \quad (10)$$

$$\text{and} \quad \nabla_{\rho} l(\theta) = 0 \quad (11)$$

For K=1, S is given as [24]

$$S = H^\dagger Z = \frac{\sum_{i=1}^N \frac{g_i (R_i - \mu_i)}{\sigma_i^2 d_i^\alpha}}{\sum_{i=1}^N \left(\frac{g_i}{\sigma_i d_i^\alpha}\right)^2}. \quad (12)$$

H^\dagger is the pseudo-inverse of matrix H [24]. The single source objective function of (9) now becomes

$$l(\theta) = \|Z - GDS\|^2 = \sum_{i=1}^N \left(\frac{R_i - \mu_i}{\sigma_i} - \frac{g_i S}{\sigma_i d_i^\alpha} \right)^2. \quad (13)$$

With initial possibility of point source to be present anywhere within the target area (point ρ_1), the value of S is calculated from (12). Then, putting this value of S in (13), value of $l(\theta)$ is obtained. The point ρ which produces least $l(\theta)$ is the estimated location of the CH₄ effusion source in the target area [24].

C. Theoretical Lower Bound of Source Estimation Error

Cramer Rao Bound (CRB) is the theoretical lower bound of the variance of an unbiased parameter estimate. It is the inverse of the Fisher information matrix. Fisher's matrix is given by [21]

$$\begin{aligned}
 J &= -E \left[\frac{\partial}{\partial \theta} \left(\frac{\partial}{\partial \theta} \ln f(Z|\theta) \right)^T \right] \\
 &= E \left\{ \left[\frac{\partial \ln f(Z|\theta)}{\partial \theta} \right] \left[\frac{\partial \ln f(Z|\theta)}{\partial \theta} \right]^T \right\}.
 \end{aligned} \quad (14)$$

Substituting (7) into equation (14), we get

$$J = \frac{\partial(DS)^T}{\partial \theta} G^T G \frac{\partial(DS)}{\partial \theta^T}, \quad (15)$$

where $\frac{\partial(DS)^T}{\partial \theta} = [B \ D]$; as $\frac{\partial(DS)^T}{\partial S} = D$, and $\frac{\partial(DS)^T}{\partial \rho_j} = B_j$.

General form of B can be found after solving from (10), (11), and (13) as [21]

$$B_k^T G(Z - HS) = 0 \quad \text{for } \{k = 1, 2, \dots, K\}, \quad (16)$$

$$\text{and} \quad B_k^T = \frac{\partial(DS)^T}{\partial \rho_k} = -\alpha S_k \begin{bmatrix} \frac{b_{1k}}{d_{1k}^{\alpha+1}} & \frac{b_{2k}}{d_{2k}^{\alpha+1}} & \dots & \frac{b_{Nk}}{d_{Nk}^{\alpha+1}} \end{bmatrix}, \quad (17)$$

where $b_{ik} = \frac{\partial d_{ik}}{\partial \rho_k} = \frac{\rho_k - r_i}{d_{ik}}$ is a unit vector from kth source to

the ith sensor. For $B = [B_1 \ B_2 \ \dots \ B_K]$, Fisher information matrix J, always nonnegative definite is [21]

$$J = \begin{bmatrix} B^T \\ D^T \end{bmatrix} G^T G \begin{bmatrix} B & D \end{bmatrix}. \quad (18)$$

Eigen decomposition of J returns the Eigen vectors and Eigen values (λ), Fig. 4. The Eigen vectors decide the direction or tilt of the 2D dilation ellipse (for K = 1) and the Eigen values determine the elliptical area of the dilation. Larger elliptical area indicates higher estimation error and vice versa. Another criterion for better estimation is the major

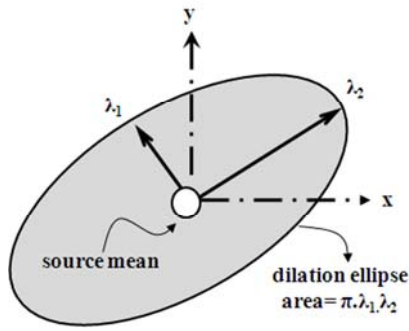


Fig. 4 CRB based estimated error dilation ellipse area determination

axis to minor axis length ratio which is termed as aspect ratio here. Aspect ratio closer to unity indicates better 2D source location estimation [25], [26].

IV. CRITERIA FOR NODE DEPLOYMENT, SUBSET SELECTION, MOBILITY OF SENSOR NODES, AND SOURCE RISK ASSESSMENT

Wireless sensor networks consist of small, low-power multisensor nodes that interact with the physical environment. The ability to add new functionality criteria to perform required measurements without physically reaching each individual sensor node is a smart and essential service, even at the limited scale [27]. In this section few such criteria are proposed that would perform precise CH₄ source localization and source threat estimation in a stepwise manner.

A. 2D Deployment Criteria for CH₄ Sensor Nodes

In order to monitor an area of interest, a large number of sensor nodes cooperate among themselves. Several physical properties can be monitored by a WSN such as temperature, humidity, pressure, ambient light, and odor concentration at distance. The collected information at sensor nodes must be integrated to identify the location of the event. Hence, sensor node positioning is a key part of successful operation of WSN [28], [29]. Optimal placement of base stations in WSN is also a very important issue. An optimal placement of base station ensures connectivity to all deployed sensor nodes within the area with minimum overall communication link distance. This geometrical issue reduces the energy consumption of sensor nodes related to data communication which in turn enhances network overall lifetime [30].

Placement of the 2D planar sensor node elements strongly affects the accuracy of the source location estimation [31]. To obtain the initial CH₄ source localization within a rectangular target area ($p_1 \times p_2$), 8 sensors (A to H) are placed elliptically around the base station or data sink Z_0 Fig. 5. For accurate single source localization in 2D, readings from at least three sensors are required. Sensing range of each sensor must be at least CZ_3 so that even if a CH₄ source is at farthest corner (like Z_3), it could be tracked (by C, D, and E nodes). CZ_3 should be greater than length m_1 and m_2 which are half of the major axis and minor axis of the sensor placement ellipse respectively Fig. 5. CRB analysis of the source localization gives minimum

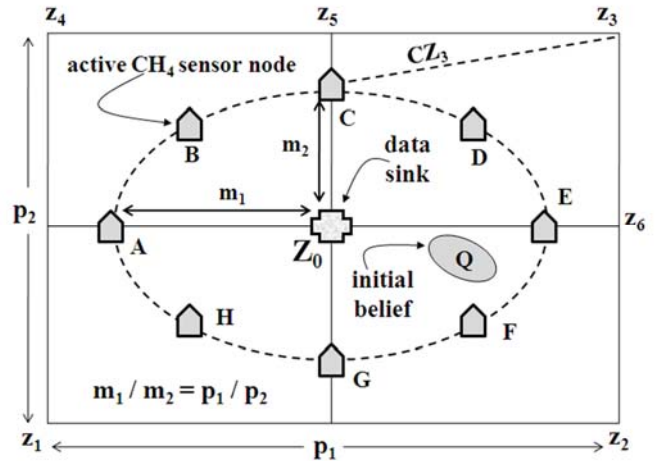


Fig. 5 CH₄ node placement criteria for initial source belief estimation

theoretical error covariance bound of the estimation. The coarse dilation ellipse, estimated at the end of the first step is termed as initial belief. For initial belief estimation, gas concentration reading from all eight sensor nodes is considered. Hence communication energy required for the initial belief estimation is found to be highest.

B. Subset Node Selection for Higher Estimation Accuracy

The main purpose of the sensor nodes with WSN is to collect local useful data and transmit them back to the base station for possible needs of further processing and data extraction [32]. These sensor nodes function in an extremely energy constrained environment. Hence, the energy usage by each node needs to be very carefully planned to have longer monitoring capability. Within an indoor environment, sensor nodes can directly transmit the data to base station.

In this second step of estimation for refinement of coarse initial belief, readings from a specific subset of nodes are only considered. This set is an optimal subset of initially used sensor nodes. It is assumed here that the subset array should contain half the number of initially used sensor nodes which are closest ones from the already estimated initial belief. Other nodes are steered into idle state to save communication energy and save network energy resources. In high uncertainty case (initial belief estimation in first case) it pays off to use all sensor node readings to estimate the source position. But in low uncertainty scenario of the second case (apriori knowledge of initial belief reduces uncertainty) a judiciously chosen subset of closest sensor nodes render more precise estimation result. It seems that for every uncertainty level (measured as the variance of noise) there is an optimal number of sensors that need to be involved in the measurement in order to achieve satisfactory results while, at the same time, be energy efficient [6].

The more precise source localization obtained in this step by using subset sensor nodes is termed as updated belief. Fig. 6 gives the pictorial view of the criteria where the initial belief is assumed to be at Q. Here, closest subset nodes D, E, F, and

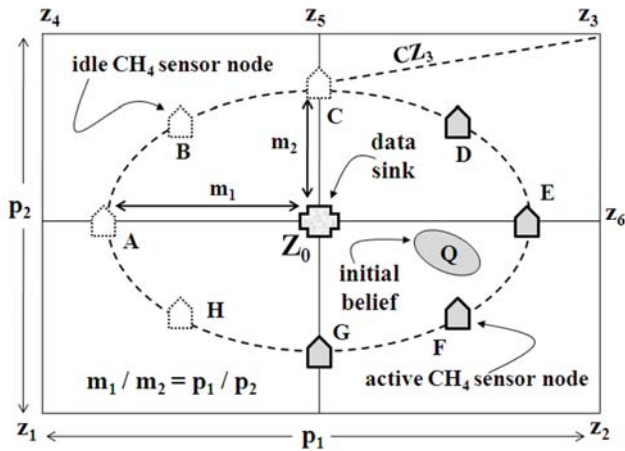


Fig. 6 CH₄ node placement criteria for initial source belief estimation

Nodes G are chosen for updated belief estimation whereas nodes A, B, C, and H go into idle state. This saves almost half of the communication energy for data transfer between nodes A, B, C, and H each to data sink Z₀. Simulation results in section VI A shows considerable improvement in updated belief estimation over initial belief are with this proposed criterion.

C. Further Refinement of Updated Estimation Belief with Limited and Directional Sensor Node Mobility

Mobility of sensor nodes within a WSN is a vast topic of research. In most of the applications, the feature of node mobility is embedded into the sensor nodes to ensure communication link connectivity between nodes or between sensor nodes and base station [33], [34]. But in our case, limited directional mobility is applied to subset sensor nodes to further enhance the precision of updated estimation belief.

Fig. 7 to Fig. 9 shows three different proposed node mobility criteria. Fig. 7 shows the criterion of subset sensor node mobility towards the major axis of the updated belief. This criterion helps to reduce the Mahalanobis distance between the measuring nodes and the covariance of the updated belief [25]. ML source localization obtained with measurements by sensor nodes at their new locations shows considerable reduction in estimation error. This belief is termed as final estimation belief. Fig. 8 shows movement of sensor nodes toward the mean of the updated belief. The criterion shown in Fig. 9 is more complicated than the previous two. Here, first the perpendicular distances to each sensor locations are calculated from the major axis and minor axis of the updated belief. Then for a particular sensor, these two distances are compared. Finally, the sensor is moved towards that axis of the updated belief which is far from the current node location. The logic is reduction of higher uncertainty between a sensor node and the updated belief. Fig. 9 shows that node SN₁ and SN₄ are comparatively far from the minor axis compared to their respective distances from the major axis of the updated belief. Hence sensors SN₁ and SN₄ are given mobility towards minor axis of the updated belief. With the same logic, node SN₂ and SN₃ are moved towards

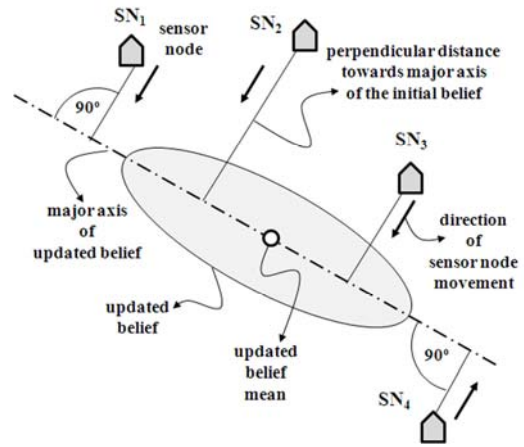


Fig. 7 node mobility towards the major axis of the updated belief

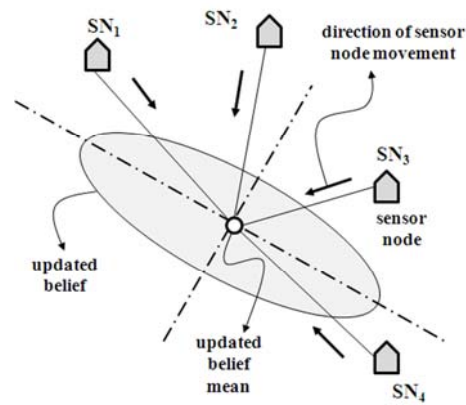


Fig. 8 directive node mobility towards the mean of the updated belief

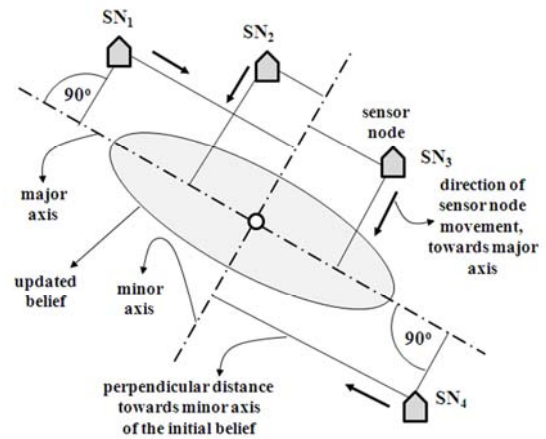


Fig. 9 node mobility towards higher uncertainty of the updated belief

the major axis of the updated belief. Directive mobility provides huge reduction in estimation uncertainty and better aspect ratio. Aspect ratio is the ratio between major axis and minor axis of the dilation ellipse. If the gas source location is within the initially placed elliptical node array, then mobility criteria incur lesser communication link length. Improvement in precision of estimation should be considerably high compared to the energy spent for successful node mobility.

D. Criteria for Remote Gas Effusion Rate Determination

The three step gas source localization process explained in previous subsections aids the remote source concentration measurement and source threat estimation process. CH_4 and H_2S gases effused from the same source have different propagation properties and hazardous effects. Presence of H_2S in air is very easily detected for its very low odor threshold. Several landfills in different parts of the United States that have been collecting large amounts of debris are installing gas processing equipment to treat H_2S concentrations in excess of 3% to 5% (30,000-50,000 ppmv) [35]. Hence, LFG source concentration ratio for CH_4 to H_2S is taken to be 45:3 or 15:1 [2]. Apart from its tendency to explode in presence of Oxygen, CH_4 is not directly as lethal as H_2S for human health. H_2S affects human health directly when its concentration in air is in the range of 10 to 50 ppm. This causes headache, nausea and breathing difficulties in human beings. H_2S concentration of 50 to 200 ppm in air causes severe conjunctivitis, acute respiratory ailment, coma, and even death in certain cases [36]. Hence it becomes important to track the concentrations of both these gases from the landfill source to mitigate their ill effects. Detailed energy model for H_2S detection with the help of WSN has been reported [37], [38].

After accurate source localization, CH_4 and H_2S effusion rate measurement from source becomes the next important job. Time varying CH_4 and H_2S concentrations readings are picked up by only one multisensor node which is nearest to the final source estimation belief (node F), Fig. 6. All remaining seven nodes are kept in idle mode during this operation. H_2S sensors should have minimum sensing range of $(z_1 z_3 / 4)$ where $z_1 z_3$ is the length of the diagonal of the rectangular target area Fig. 6. Using the remote steady state readings of CH_4 and H_2S concentrations at node F, and the known propagation constants of both these gases, their concentration ratio is estimated at source. Lesser the ratio, higher would be the H_2S based threat possessed by the LFG source [39]. Calculation for source threat estimation is explained in section VI C with the help of remote gas concentration graph and values obtained at closest node.

V. INDOOR GAS SOURCE LOCALIZATION BY 3D WSN IN PRESENCE OF OBSTRUCTION IN GAS PROPAGATION PATH

Indoor gas source localization and risk assessment criteria explained so far did not consider any obstruction in the gas propagation path. The 2D WSN placed on the floor losses its effectiveness in presence of an obstruction on floor. In such cases the initial gas source domain estimation can be carried out by placing sensor nodes in the ceiling. This is a common practice in non-cooperative environmental monitoring. Many environmental factors, such as the presence of pyrophoric CH_4 and other hazardous gases, water, and dust need be monitored in long and narrow underground tunnels to ensure safe working conditions for coal miners. Here, stationary sensor nodes are deployed on the walls and ceiling of tunnels to form a mesh sensor network [40]. In a mobile robot and sensor

node based hybrid navigational system, sensor nodes attached to the ceiling act as signposts to guide the robot along the routing path on floor. The ceiling sensors inform the ground based robot of the next node that it has to pass through. The robot exchanges distance information with each ceiling sensor nodes and follows along the routing path on ground [41].

For CH_4 source localization with obstacles on basement floor, eight planar sensor nodes are fixed to the ceiling in same elliptical fashion as in Fig. 5. As CH_4 is a light gas, after effusion it would reach the unobstructed ceiling in a short span of time. Ceiling based concentration measurements also produce authentic source localization. CH_4 concentration readings picked up by the ceiling sensor nodes are transmitted to the base station. ML based source localization is carried out with these readings at base station to obtain coarse initial belief at ceiling. The belief is then projected back on the floor. CRB based initial belief is found to have very large dilation area. It happens because gas concentration signal strengths obtained at ceiling are far less than that on basement floor.

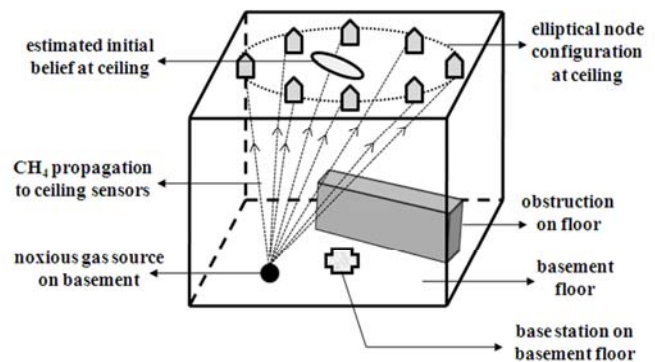


Fig. 10 source localization with obstacle by 3D sensor networks

From this first step, the relative position of the gas source on floor is successfully determined with respect to the obstacle, Fig 10. The direction of the CH_4 distribution is also found from this step. With these two apriori information, in the next step, a planar elliptical network with judiciously chosen four sensor nodes are placed on the floor for updated belief estimation. The sensor nodes on the floor are to be deployed according to the criteria explained in section IV B keeping position of obstruction into consideration. Criteria for node mobility and selection of a single sensor node for remote determination of gas concentration ratio at source would follow next. Results and related assumptions explained in section VI D strongly validates this 3D sensor network based CH_4 source localization process in presence of obstacles on floor. The impact of wind flow is not considered in this case.

VI. RESULTS AND DISCUSSION

In this section, simulation results and related analysis are discussed with the help of graphs and tables. Simulations have been performed using MATLAB version 7.9. Following are the results for the representative cases.

A. 2D Node Based CH₄ Source Updated Belief Estimation

For simulation based localization of the CH₄ gas source within a 100×80 square unit rectangular area, an elliptically placed planar network of eight sensor nodes (A to H) has been considered. One unit corresponds to 0.1 meter. The assumed sensor node coordinates are shown in Fig. 11. The gas source is assumed to be at [55, 45]. The base station is at [50, 40] which is also the centre of the target area. The source energy is set as 4000 and background noise is set at $\mu_i = 2.3$ for all sensor nodes. The noise energy variation $\epsilon_i(t)$ is modeled as a Gaussian random variable $N(\mu_i, 2\mu_i^2/M)$ with $M = 30$. Objective function reduction result for initial belief estimation is shown in Fig. 12. The least value of objective function was obtained at coordinate [55, 47]. This is the most likely position of the CH₄ source obtained by using the measured readings of gas concentration at all eight sensor nodes. The estimated source position is 2 units off from the assumed source position. CRB based estimation analysis shows initial belief dilation area to be very wide 78.1 square units, Table I. It indicates large source localization error. This error is minimized next by judiciously selecting four sensor nodes closest to the initially estimated belief (case 2, Table I). Now the CH₄ concentration readings only from node B, C, D, and E are considered and again ML based source localization is carried out, Fig. 13. CRB based updated belief dilation area obtained after the second case is reduced by 61.5% than that in case 1, Table I. Aspect ratio of 4.26 of initial belief is improved to 3.44 during updated belief estimation.

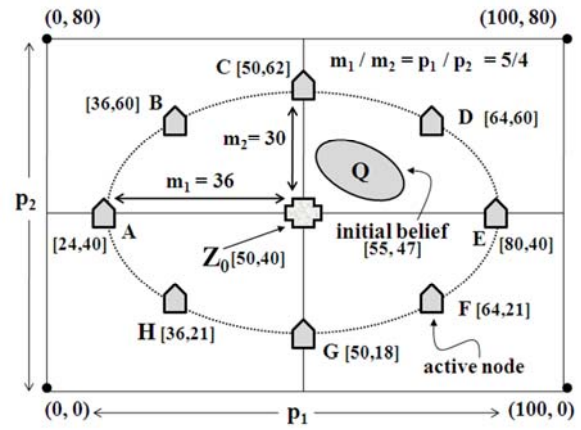


Fig. 11 2D sensor placement for initial belief estimation by 8 sensors

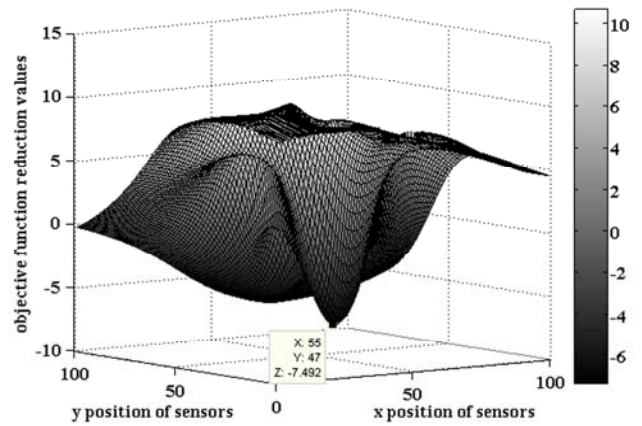


Fig. 12 objective function reduction for initial belief estimation

TABLE I

% IMPROVEMENT IN PERFORMANCE PARAMETERS (COMPARED TO CASE 1) FOR ALL DIFFERENT SENSOR NODE CONFIGURATIONS

| Case | Sensor Node Geometry | Dilation Area Sq. Units | Aspect Ratio | Link Length Units |
|------|--|-----------------------------|-----------------------------|------------------------------|
| 1 | 8 sensor nodes | 78.1 | 4.26 | 200 |
| 2 | 4 closest sensor nodes no node mobility | 30.1 61.5% | 3.44 19.2% | 100 50% |
| 3 | 4 closest nodes, 1 unit mobility towards major axis | 9.3 88 % | 3.34 21.6% | 98.2 51% |
| 4 | 4 closest nodes, 1 unit mobility towards mean | 8.44 89.2% | 3.57 16.2% | 96.8 51.6% |
| 5 | 4 closest nodes, 1 unit mobility towards higher uncertainty | 8.98 88.5% | 3.25 23.7% | 97.25 51.4% |
| 6 | 4 closest nodes, 2 units mobility towards major axis | 2.96 96.2% | 3.15 26% | 95.6 52.2% |
| 7 | 4 closest nodes, 2 units mobility towards mean | 2.6 96.7% | 3.7 13.1% | 92.93 53.5% |
| 8 | 4 closest nodes, 2 units mobility towards higher uncertainty | 2.8 96.4% | 3 29.5% | 93.74 53.1% |

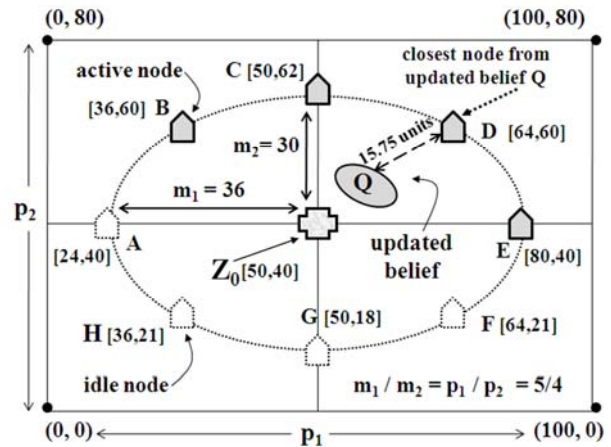


Fig. 13 optimal subset node selection for updated belief estimation

B. Final Belief Estimation with Limited Node Mobility

After judicious selection of subset nodes and after carrying out the updated belief estimation, limited mobility of one unit and two units are applied to the subset sensor nodes in steps. Node mobility towards a predefined direction logically reduces the estimated final belief area and hence offers very high degree of precision in source position estimation. Among

the three mobility criteria it is found that ‘node mobility towards estimated mean of the source’ (case 4, Table I) provides most precise source localization. For this, the third column results of third fourth and fifth rows of Table I are compared. Case 4 shows as much as 89.2% reduction in estimation belief as compared to that of case 1, Table I. It is also observed from fifth row of Table I that ‘mobility toward higher uncertainty direction of updated belief’ provide best aspect ratio of final belief estimation. The aspect ratio of 4.26 in the first case has been improved to best 3.25 using this criterion. New node positions after ‘mobility of 1 unit toward mean direction’ (case 4, Table I) are depicted in Fig. 14.

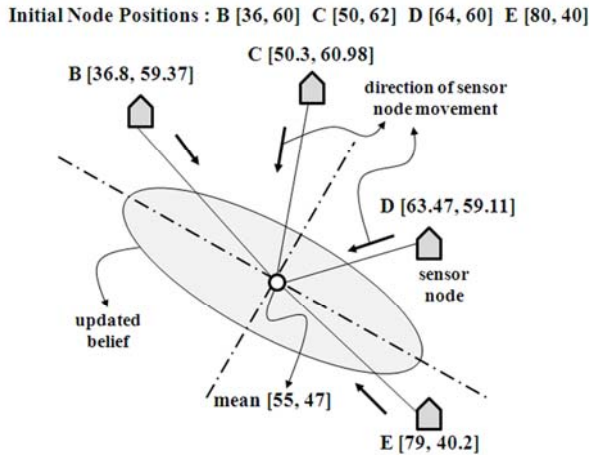


Fig. 14 one unit mobility towards mean of the updated belief

Important observations regarding overall communication link length and network energy resource optimization were made from Table I. The 8 communication links with base station in case 1 (Fig. 11) is reduced to only 4 links in the case 2 (Fig. 13). This saves 50% communication energy in case 2. At the same time it enhances the estimation accuracy by reducing dilation ellipse area by 61.5% compared to case 1. The results validate the proposed subset node selection criteria. Link length reduction is minimal due to limited mobility in sensor nodes. This is highly subjective and totally depends upon the relative position between updated belief and the subset sensor node positions. In our example, the criterion of ‘node mobility towards mean’ (case 4, Table I) shows minimum communication link length during final belief estimation and hence maximum network energy saving.

C. Gas Source Risk Assessment Analysis

Simulation for measurements of remote gas concentration from a mixed gas source has the basic assumption that CH₄ and H₂S are emitted from the same source at a constant rate. As the source concentration of H₂S is generally low and as the concentration gradient of H₂S falls sharply, far away H₂S sensors from source are found to generate more noise. They do not generate reasonable gas concentration readings. This adds to estimation inaccuracies. Hence only the closest H₂S sensor measurements are considered for remote source threat analysis purpose. It is evident that the accuracy of the source

localization process is the most important factor in selection of that very closest H₂S sensor node which would remotely track the time varying H₂S concentration most accurately.

From Fig. 13 it is found that sensor node D of the optimal subset is the closest (DQ Euclidean distance = 15.75 units) from the mean of the updated belief. After 1 unit mobility of the subset nodes towards updated belief mean, DQ (referred as ‘d’) reduces to 14.75 units, Fig. 14. By using experimental setup of Fig. 1, time varying CH₄ and H₂S concentrations were picked up at distance of 14.75 units from the mixed gas source. As the tracking took place within the test bed, the effects of wind velocity did not affect the measurements. We found that the CH₄ sensor attained the steady state lot earlier than H₂S sensor, Fig. 15. It happened because CH₄ travels faster with a lesser propagation constant than H₂S. Fig 15 shows that the steady state CH₄ as to H₂S ratio at distance of 14.75 units from source is 1 : 0.237 after 300s. Actual CH₄ to H₂S concentration ratio at source is now back calculated using gas propagation constants of gases as

$$\begin{aligned} & \text{CH}_4 \text{ to H}_2\text{S gas concentration ratio at source} \\ &= (d^{\alpha_{\text{H}_2\text{S}}} / d^{\alpha_{\text{CH}_4}}) \times (\text{steady state CH}_4 : \text{H}_2\text{S ratio at 14.75} \\ & \quad \text{units distance from mixed gas source}) \\ &= (14.75^{2.60} / 14.75^{2.30}) \times (1 / 0.237) \\ &= 9.46 : 1 \end{aligned}$$

As this ratio is 37% less than the standard LFG CH₄ to H₂S ratio (which is 15:1), the source is considered to be highly dangerous from noxious H₂S gas based hazards point of view and requires faster intervention.

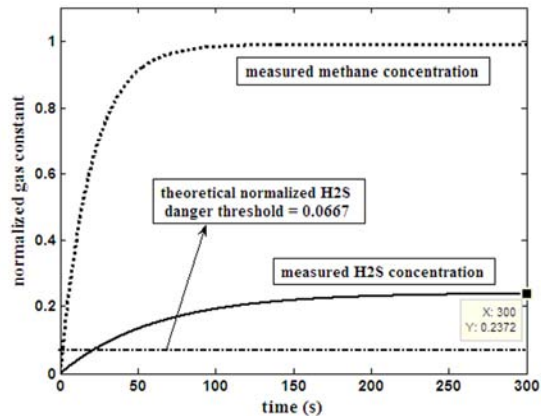


Fig. 15 remote CH₄ and H₂S concentration measurement over time

D. Source Localization with Obstacles using 3D Nodes

The result for 3D ceiling and ground node based source belief estimation is explained here. The assumed position of obstacle on ground with respect to the initially configured elliptical node array is shown in Fig. 16. Elliptical placement of sensor nodes on ground (as shown in Fig. 11) is impractical as source position with respect to the obstacle is initially unknown. For gas concentration measurement at ceiling, sensor coordinates of Fig. 11 are placed onto ceiling with a third dimension of 30 which is the assumed height of the room. Hence sensor A coordinate at ceiling is now [24, 40, 30], coordinate of ceiling sensor B becomes [36, 60, 30], and

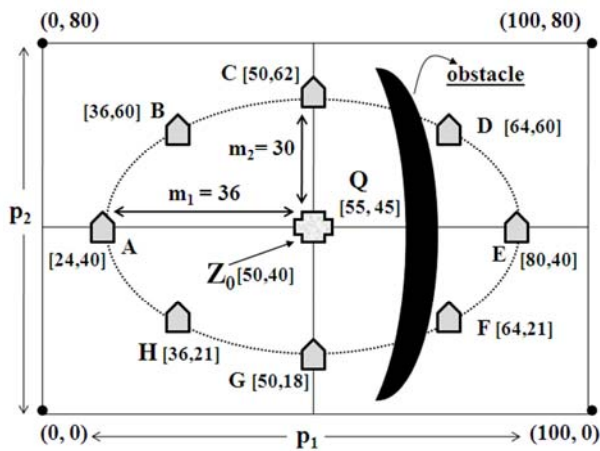


Fig. 16 obstacle on ground with initial elliptical ground node array

so on. Base station is at $[50, 40, 0]$. CH_4 source coordinate is assumed at $[55, 45, 0]$ on floor. The objective function reduction (3D) at ceiling for source domain estimation is shown in Fig. 17. At ceiling the estimated mean is at $[56, 46]$. For this estimation source and noise assumptions are kept same as mentioned in section VI A. An important fact here is

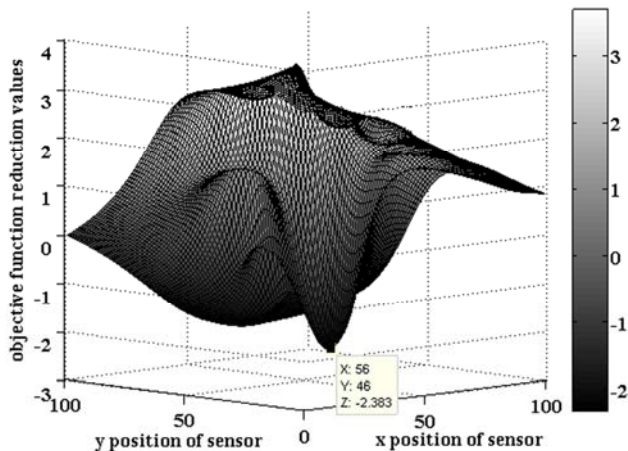


Fig. 17 objective function reduction by ceiling based measurements

that all the received signal strengths at ceiling sensor nodes are given a gain (g) of 2.8. The mean value is then projected on the ground which falls in the left side of the obstruction shown in Fig. 16. CRB based error estimation is carried out next which shows very wide dilation area of 516 sq. units. The large dilation error is caused by very weak received signal strength at the ceiling sensor nodes. But the direction of the gas distribution is found from this CRB estimation. In next step, a planar sensor node is deployed in the left side area of the obstacle and the initial belief area is reduced to determine the updated belief. Directional node mobility and source risk assessment can be carried next as explained in IV C and IV D.

VII. CONCLUSION

This work explains a novel remote and proximity probe approach for 2D and 3D ad-hoc WSN based hazardous gas

source detection and threat estimation technique. The mathematical model explained here enhances speed of gas effusion source localization for multiple sources. Simulation results show that probability of success for precise source detection increases with proper selection of sensor nodes. It also produces a more meaningful measurement reading which adds to the localization accuracy. The remote gas concentration estimation at source and its risk assessments are carried out without much complexity. Propagation constant of respective gases in the media is deduced experimentally.

Future works include CO_2 source detection and tracking as CO_2 is another dominant landfill gas. Higher CO_2 concentration in a closed environment also has severe adverse effects on human health. Apart from that, VOC threat analysis of the LFG source can be also carried out. Remote source localization and gas concentration determination at source in a constrained 3D environment in presence of environmental nonlinearities like wind flow, temperature, and humidity is also another work to be carried out in future.

ACKNOWLEDGMENT

We express our sincere thanks to Crompton Greaves Limited, Mumbai for sponsoring the research work.

REFERENCES

- [1] Amiya Kumar Sahu, "Present scenario of municipal solid waste (MSW) dumping grounds in India," *Proceedings of the International Conference on Sustainable Solid Waste Management*, Chennai, India, pp. 327 – 333, September 2007.
- [2] <http://www.odh.ohio.gov/ASSETS/95EF6FEF9DD346079C1C72C4FD72254E/LandfillGas.pdf>
- [3] David Fischer, and Christopher G. Urchin, "Laboratory simulation of VOC entry into residence basements from soil gas," *Journal of Environmental Science and Tech.*, vol. 30, issue 8, pp. 2598 – 2603, July 25, 1996.
- [4] <http://www.cbc.ca/news/world/story/2010/11/14/mexico-hotel-explosion.html>
- [5] John-Won Kwon, Young-Man Park, Sang-Jun Koo, and Hiesik Kim, "Design of air pollution monitoring system using ZigBee networks for ubiquitous-city," in *Proceedings of IEEE Int. Cnfrnc. on Convergence Information Technology*, Korea, pp. 1024 – 1031, November 2007.
- [6] Michalis P. Michaelides, and Christos G. Panayiotou, "Plume source position estimation using sensor networks," *Proceedings of IEEE 13th Mediterranean Conf. on Control and Automation*, Cyprus, pp. 731 – 736, June 27-29, 2005.
- [7] Wilfrid Bourgeois, Anne-Claude Romain, Jacques Nicolas, and Richard M. Stuetz, "The use of sensor arrays for environmental monitoring: interests and limitations," *Journal of Environmental Monitoring Critical Review*, vol. 5, pp. 852 – 860, 2003.
- [8] Winsu Jatimiko, Kosuke Sekiyama, and Toshio Fukuda, "A PSO-Based mobile robot for odour source localization in dynamic advection-diffusion with obstacles environment: theory, simulation and measurement," *IEEE, Computational Intelligence Magazine*, Volume: 2, Issue: 2, 2007, pp. 37 – 51.
- [9] X. Cui, C.T. Hardin, R.K. Ragade, and A.S. Elmaghraby, "A swarm-based fuzzy logic control mobile sensor network for hazardous contaminants localization," *Proc. of IEEE International Conference on Mobile Ad-hoc and Sensor Systems (MASS)*, pp. 194–2002, 2004.
- [10] M. Wandel, A. Lilienthal, T. Duckett, U. Weimar, and A. Zell, "Gas distribution in unventilated indoor environments inspected by a mobile robot," *Proc. of IEEE International Conference on Advanced Robotics (ICAR)*, pp. 507–512, 2003.
- [11] A. Jeremić, and Arye Nehorai, "Landmine detection and localization using chemical sensor array processing," *IEEE Transaction on Signal Processing*, vol. 48, no 5, pp. 1295 – 1305, May 2000.

- [12] Arye Nehorai, Boaz Porat, and Eytan Paldi, "Detection and localization of vapour-emitting sources," *IEEE Transaction on Signal Processing*, vol. 43, no. 1, pp. 243 – 253, January 1995.
- [13] Hiroshi Ishida, Yukihiko Kagawa, Takamichi Nakamoto, and Toyosaka Morrizumi, "Odor-source localization in the clean room by an autonomous mobile sensing system," *Elsevier Sensors and Actuators Journal*, B 33, pp. 115 – 121, 1996.
- [14] Xiaojun Zhang, and Minglu Zhang, "Biologically-inspired search strategy for locating odor source," *Proceedings of IEEE Fourth International Conference on Natural Computation*, Volume 4, 2008, pp. 342 – 346.
- [15] Hua Wang, Yiming Zhou, Xianglong Yang, and Liren Wang, "Plume Source Localizing in Different Distributions and Noise Types Based on WSN," *Proceedings of IEEE International Conference on Communications and Mobile Computing*, Volume 3, 2010, pp. 63 – 66.
- [16] Mohammad Reza Akhondi, Alex Talevski, Simon Carlsen, and Stig Petersen, "Applications of wireless sensor networks in the oil, gas and resources industries," in *Proceedings of 24th IEEE International Conference on Advanced Information Networking and Applications*, Perth Australia, pp. 941 – 948, 10-13 April 2010.
- [17] Chao Xiaojuan, Walteneug Dargie and Lin Guan, "Energy model for H₂S monitoring wireless sensor network," in *Proceedings of 11th IEEE International Conference on Computational Science and Engineering*, São Paulo, Brazil, pp. 402 – 409, 16-18 July 2008.
- [18] A. W. Harris, A. Atkinson, and P. A. Claisse, "Transport of Gases in Concrete Barriers," *Science Direct Journal of Waste Management*, Vol. 12, Issues 2-3, 1992, pp. 155 – 178.
- [19] Abdalla M. Odeh, Wa'il Abu-El-Sha'r, and Rami Al-Ruzouq, "Gas transport through concrete slabs," *Elsevier Journal of Building and Environment*, vol. 41, 2006, pp. 492–500.
- [20] Yves F. Houst, and Folker H. Wittmann, "Influence of porosity and water content on the diffusivity of CO₂, and O₂ through hydrated cement paste," *Pergamon Journal of Concrete Research*, vol. 24, no. 6, pp. 1165 – 1176, 1994.
- [21] Xiaohong Sheng and Yu-Hen Hu, "Maximum likelihood multiple-source localization using acoustic energy measurement with wireless sensor networks," *IEEE Transactions on Signal Processing*, vol. 53, no. 1, pp. 44 – 53, January 2005.
- [22] Majid Mohamady Oskouei, and Rashed Poormirzaee, "Detection of the Number of Signal Sources in the Hyperspectral Data," *NAUN International Journal of Circuits, Systems, and Signal Processing*, vol. 3, issue 4, 2009, pp. 190-197.
- [23] Rung-Ching Chen, and Sheng-Ling Huang, "a new method for location based on radio frequency identification," *WSEAS Transactions on Communications*, Vol. 8, issue 7, July 2009, pp. 618-627.
- [24] Noriaki Kitakoga, and Tomoaki Ohtsuki, "Distributes EM algorithms for acoustic source localization in sensor networks," *Proceedings of IEEE Conference on Vehicular Technology*, pp. 1 – 5, 2006.
- [25] F. Zhao, J. Shin, and J. Reich, "Information-driven dynamic sensor collaboration for tracking applications," *IEEE Signal Processing Magazine*, vol. 19, issue 2, March 2002, pp. 61 – 72.
- [26] Erik G. Larsson, "Cramer-Rao bound analysis of distributed positioning in sensor networks," *IEEE Signal Processing Letters*, vol. 11, no. 3, pp. 334 - 337, March 2004.
- [27] Thanos Stathopoulos, John Heidemann, and Deborah Estrin, "A Remote code update mechanism for wireless sensor networks," *CENS Technical Report # 30*, Centre for Networked Sensing, USC/Information Sciences Institute, pp. 1-15.
- [28] Zoran Bojkovic, and Bojan Bakmaz, "A survey on wireless sensor networks deployment," *WSEAS Transactions on Communications*, vol. 7, issue 12, December 2008, pp. 1172-1181.
- [29] Vitaliy Rybak, "Environment infrastructure and multi-sensor integration for autonomous service robotics," *NAUN International Journal of Circuits, Systems, and Signal Processing*, vol. 5, issue 3, 2011, pp. 201-211.
- [30] B. Paul, M. A. Matin, M. J. Showkat, and Z. Rahman, "Optimal placement of base stations in a two tiered wireless sensor network," *WSEAS Transactions on Communications*, vol. 9, issue 1, January 2010, pp. 43-52.
- [31] Baysal U., and R. L. Moses, "On the geometry of isotropic arrays," *IEEE Transactions on Sig. Proc.*, vol. 51, no. 6, pp. 1469-1478, June 2003.
- [32] Tung-Jung Chan, Ching-Mu Chen, Yung-Fa Huang, Jen-Yung Lin, and Tair-Rong Chen, "Optimal cluster number selection in ad-hoc wireless sensor networks," *WSEAS Transactions on Communications*, vol. 7, issue 8, august 2008, pp. 837-846.
- [33] Radu Dobrescu, Dan Popescu, and Maximilian Nicolae, "Mobile node implementation for WSN applications," *NAUN Intrntnl. Journal of Circuits, Systems, and Signal Proc.*, vol. 2, issue 2, 2008, pp. 121-30.
- [34] Paolo Di Giamberardino, Ivano Bergamaschi, and Andrea Usai, "A local information based protocol for networks data exchange with application to mobile sensor networks," *WSEAS Transactions on Communications*, vol. 8, issue 8, August 2009, pp. 795-804.
- [35] http://www.merichem.com/resources/technical_papers/municipal_landfill_ls.php
- [36] http://www.safetydirectory.com/hazardous_substances/hydrogen_sulfide/fact_sheet.htm
- [37] Chao Xiaojuan, Walteneug Dargie and Lin Guan, "Energy model for H₂S monitoring wireless sensor network," in *Proceedings of 11th IEEE International Conference on Computational Science and Engineering*, São Paulo, Brazil, pp. 402 – 409, 16-18 July 2008.
- [38] Mohammad Reza Akhondi, Alex Talevski, Simon Carlsen, and Stig Petersen, "Applications of wireless sensor networks in the oil, gas and resources industries," in *Proceedings of 24th IEEE International Conference on Advanced Information Networking and Applications*, Perth Australia, pp. 941 – 948, 10-13 April 2010.
- [39] Saurav Mitra, Kushal Tuckley, and Siddhartha Duttgupta, "Localization and threat estimation of noxious gas source originating from buried landfills," *Proceedings of NAUN / WSEAS International Conference. USCUDAR 2011*, Prague, Czech Rep., Septmbr. 2011, pp. 148-154.
- [40] Mo Li, Mo Li, and Yunhao Liu, "Underground structure monitoring with wireless sensor networks," *Proceedings of IEEE ISPN'07*, April 25-27, Cambridge, Massachusetts, 2007, pp. 69-78.
- [41] Heesung Chae, Wonpil Yu, Jaeyeong Lee, and Young-Jo Cho, "Robot localization sensor for development of wireless location sensing network," *Proceeding of the IEEE Int. Conference, Intelligent Robots and Systems*, Beijing, China, October 2006, pp. 37-42.



Saurav Mitra, born in Basirhat, West Bengal, India, received Bachelor in Engineering degree in electronics from Shivaji University and M-Tech degree in instrumentation from SRTM University, Maharashtra, India respectively in 1999 and 2006. Currently he is pursuing Ph. D. in electrical engineering in Indian Institute of Technology Bombay (IIT Bombay).

He was an assistant professor in the department of electronics and telecommunication engineering in RMCET, Ratnagiri, Mumbai University. He has published and presented in seven national and international conferences. His research interests include sensor networks based event localization, digital signal processing, statistical signal processing, power optimization from renewable energy sources, and fuel cell degradation monitoring.



Kushal Tuckley, born in Mumbai, India, received B. Tech degree in electrical engineering from IIT Bombay in 1985. He received M-Tech and Ph.D. degrees from the same institute respectively in 1989 and 2009. His major field of study has been communication engineering.

Dr. Tuckley is currently the chairman and head of research and development group of AGV systems Private Limited, Mumbai, India. Since September 1985 he was with SAMEER, Mumbai as Scientist and left the institute in March 2010 as Head, Signal Processing and Navigational Electronics Division. As project manager in SAMEER, he has completed and coordinated many projects like Automation of Lighthouses in Saurashtra and Kuchchh region in Gujarat, Radar Beacon for ship navigation, and so on. He has published and presented in twenty national and international conferences. His research interests include digital and RF signal processing, RF and microwave communication, radar based communication, and system engineering.



Siddhartha P. Duttagupta obtained B.Tech.-Honours degree from IIT Kharagpur, India in 1991. He received Ph.D. from the University of Rochester, Rochester, New York, USA in 1998.

He was a faculty member at Boise State University, Boise, Idaho, USA from 1997-2002, and at the IIT Bombay, India from 2002 onwards. Here where he is currently an Assistant Professor. He was also associated with the private sector, primarily in sectors of renewable energy and nanotechnology.

Dr. Duttagupta has research interests in the area of micro-system design and micro/nano process optimization. Currently his research contribution can be measured in terms of a significant citation impact (> 1000) and an H-index of 12. He has published and presented over 33 papers, and acted as a referee for leading international journals. He also has been awarded two Indian patents and has authored two books. Dr. Duttagupta has been involved with multiple sponsored projects from agencies based in India and in the USA in the capacity of principal and co-investigator.



Samsul Ekram obtained his Bachelor in Engineering degree in electrical from the Bengal Engineering College, Shivpur, West Bengal, India in 1993 and the Master in Engineering degree and Ph.D. from the SGS Institute of Technology and Science, Indore, India respectively in 1997 & 2007. He was postdoctoral fellow in the Department of Systems and Naval Mechatronics Engineering, National Cheng Kung University (NCKU), Tainan, Taiwan in 2008.

Dr. Ekram is currently the Assistant General Manager of Electronics Design Centre at Global Research and Development Centre, Crompton Greaves Ltd. Kanjurmarg (East), Mumbai, India. He has research interests in the area of Power Electronics for Motion Control and Power Quality. He has published and presented over 23 papers and acted as referee for leading international journals. He also has been awarded one Indian patent and filed 19 more in last three years. The filed patents are now under examination process.